Development 135, 3355-3367 (2008) doi:10.1242/dev.022830

odd skipped related1 reveals a novel role for endoderm in regulating kidney versus vascular cell fate

Sudha P. Mudumana[1], Dirk Hentschel[2], Yan Liu[1], Aleksandr Vasilyev[1] and Iain A. Drummond[1,*]

The kidney and vasculature are intimately linked both functionally and during development, when nephric and blood/vascular progenitor cells occupy adjacent bands of mesoderm in zebrafish and frog embryos. Developmental mechanisms that underlie the differentiation of kidney versus blood/vascular lineages remain unknown. The *odd skipped related1* (*osr1*) gene encodes a zinc-finger transcription factor that is expressed in the germ ring mesendoderm and subsequently in the endoderm and intermediate mesoderm, prior to the expression of definitive kidney or blood/vascular markers. Knockdown of *osr1* in zebrafish embryos resulted in a complete, segment-specific loss of anterior kidney progenitors and a compensatory increase in the number of angioblast cells in the same trunk region. Histology revealed a subsequent absence of kidney tubules, an enlarged cardinal vein and expansion of the posterior venous plexus. Altered kidney versus vascular development correlated with expanded endoderm development in *osr1* knockdowns. Combined *osr1* loss of function and blockade of endoderm development by knockdown of *sox32/casanova* rescued anterior kidney development. The results indicate that *osr1* activity is required to limit endoderm differentiation from mesendoderm; in the absence of *osr1*, excess endoderm alters mesoderm differentiation, shifting the balance from kidney towards vascular development.

KEY WORDS: Odd-skipped related, Endoderm, Pronephros, Vasculature, Glomerulus, Kidney development, Zebrafish

INTRODUCTION

The kidney and vasculature are mesodermal derivatives that originate from adjacent regions of gastrulating fish and frog embryos (Iraha et al., 2002; Kimelman, 2006; Kimmel et al., 1990; Walmsley et al., 2002). Soon after gastrulation is complete, zebrafish kidney progenitors, which are marked by the expression of transcriptional regulators such as *pax2a* (Krauss et al., 1991; Majumdar et al., 2000) and *lim1* (Toyama and Dawid, 1997), and blood/vascular progenitors, which are marked by expression of *scl* (Gering et al., 1998) and *gata1* (Detrich et al., 1995), are found in adjacent stripes of mesoderm lateral to the somites. These tissues, referred to as intermediate mesoderm (IM) in nephric development and lateral plate mesoderm (LPM) in blood vascular development, serve as the source of all pronephric cells, the posterior blood islands, and the main vessels of the trunk, the dorsal aorta and the cardinal vein. Analysis of mesoderm patterning in frog embryos has demonstrated overlapping expression of the vascular marker *fli1* and the kidney marker *lim1* in intermediate mesoderm (Walmsley et al., 2002), suggesting that, prior to cell differentiation, kidney and blood/vascular cells may share a common progenitor cell population. The close association of kidney and vascular progenitor cells during development is ultimately manifested as a functional relationship in the mature organs, where arterial blood is filtered by the kidney glomerulus and metabolites recovered by kidney tubules are delivered directly back to the venous blood supply. This relationship between kidney and vascular tissues raises the idea that the specification of kidney and vascular progenitor cells in early embryos may be influenced by common developmental regulatory factors.

Both kidney and vascular patterning is strongly influenced by bone morphogenetic proteins (BMPs) during gastrulation (Kimelman, 2006; Kimelman and Griffin, 2000; Pyati et al., 2005; Stickney et al., 2007; Szeto and Kimelman, 2004). Zebrafish mutants defective in BMP signaling, such as *swirl/bmp2b* (Kishimoto et al., 1997; Nguyen et al., 1998), *snailhouse/bmp7* (Dick et al., 2000; Schmid et al., 2000) and *somitabun/smad5* (Hild et al., 1999), show a reduced number of both kidney and blood cell progenitors, and an expansion of dorsal somites. However, ventralized/posteriorized mutants that lack BMP inhibitors such as *chordino/chordin* and the tolloid antagonist *ogon/sizzled* show an enlargement of kidney and blood precursor cell populations and a loss of anterior somites (Hammerschmidt et al., 1996; Leung et al., 2005; Miller-Bertoglio et al., 1999). Signaling events occurring later in development may also affect kidney versus blood/vascular fates. Post-gastrulation expression of a dominant-negative BMP receptor expands the *gata1*-positive blood progenitor cell population and reduces the number of *pax2a*-positive kidney progenitor cells in the ventroposterior mesoderm (Gupta et al., 2006). Mutations in BMP4 affect ventrolateral mesoderm at post-gastrulation stages, favoring blood and kidney development at the expense of vascular development (Stickney et al., 2007). Evidence has also been presented that blood/vascular and kidney fates may be mutually exclusive in the mesoderm. Ectopic overexpression of the blood/vascular transcriptional regulators *scl* and *lmo2* during early development results in expansion of the blood/vascular progenitor cell population at the expense of kidney progenitors, indicating that intermediate mesoderm can be transfated to blood/vasculature mesoderm (Gering et al., 2003). These findings suggest that the differentiation of the blood/vascular and kidney lineages are linked at multiple stages of development. It is likely that, in addition to BMP signaling, other morphogens and transcriptional circuitry is required to ultimately define lateral mesoderm cell lineages.

The zinc-finger transcription factor *odd-skipped related 1* (*osr1*) is initially expressed in the mesendoderm in gastrulating zebrafish embryos and, later, in a broad domain of lateral plate/intermediate

[1]Nephrology Division, Massachusetts General Hospital, Charlestown, MA 02129, USA. [2]Renal Division, Brigham and Women's Hospital, Boston, MA 02115, USA.

*Author for correspondence (e-mail: idrummon@receptor.mgh.harvard.edu)

Accepted 26 August 2008

mesoderm that encompasses both kidney and vascular mesoderm in chick, mouse and zebrafish embryos (James et al., 2006; Tena et al., 2007; Wang et al., 2005). Mouse embryos lacking a functional *Osr1* gene show cardiac defects and kidney agenesis (James et al., 2006; Wang et al., 2005). Knockdown experiments in zebrafish have also revealed a role for *osr1* in pronephric development (Tena et al., 2007). We present here evidence that *osr1* is not only required for zebrafish kidney development but that it also controls the commitment of mesoderm to the angioblast cell fate. Surprisingly, we find that the function of *osr1* in post-gastrulation mesoderm differentiation is linked to an early role in regulating mesoderm versus endoderm differentiation during gastrulation. Our findings reveal a novel role for endoderm in determining the balance of kidney versus angioblast cell differentiation during somitogenesis.

MATERIALS AND METHODS

Plasmid constructs

The zebrafish *osr1* gene was identified by tblastn search of zebrafish genomic DNA sequence (Sanger Center zebrafish genome project; http://www.sanger.ac.uk/Projects/D_rerio/) using mouse Osr1 protein sequence as query. Reverse blastx using zebrafish *osr1* coding sequence as query against GenBank confirmed the zebrafish gene as the closest *osr1* ortholog. Full-length *osr1* was amplified by RT-PCR from RNA obtained from 24 hpf wild-type Tü/AB embryos and cloned into pCR4 vector. Additional plasmid probes (*lim1*, *pax2a*, *pax8*, *nbc1*, *nephrin*, *wt1a*, *ae2*, *myoD*, *ret1*, *scl*, *gata1*, *flk1*, *nkx2.5*, *etsrp1*, *pu.1* and *trpm7*) have been previously described. Synthetic capped mRNAs for rescue experiments were synthesized from linearized full-length plasmid constructs using mMessage Machine kit (Ambion, USA). Specifically, *pax2a* mRNA and *osr1* mRNA was obtained by *in vitro* transcription with *sp6* polymerase from a *Not*I-linearized and a *Kpn*I-linearized full-length construct, respectively.

Zebrafish embryos

Wild-type zebrafish were maintained according to established protocols (Westerfield, 1995). The embryos for experiments were collected from crosses of wild-type Tü/AB adults, grown at 28°C and fixed at the indicated developmental stages. *bonnie and clyde* homozygous mutant embryos were obtained from an incross of $bon^{m425/+}$ heterozygotes.

Morpholino antisense oligonucleotides

Morpholino oligonucleotides were designed to either target the translation start site or the splice donor site of target mRNAs. The following morpholino oligonucleotides were used: *osr1* ex2d (*osr1*MO), ATCTCATCCTTACCTGTGGTCTCTC; *osr1* ATG, GGAGCGTCTTACTACCCATGACTAA; *osr1*CoMO, AATCAGTACCCATCATTCTGCGAGG; *scl* ATG, GCTCGGATTTCAGTTTTTCCATCAT (Sumanas and Lin, 2006); *pax2a* E2, TATGTGCTTTTTCTTACCTTCCGAG; *pax8* E5, TTTCTGCACTCACTGTCATCGTGTC (Hans et al., 2004); *pax8* E9, ACCGGCGGCAGCTCACCTGATACCA (Hans et al., 2004); *sox32* ATG, CAGGGAGCATCCGGTCGAGATACAT (Dickmeis et al., 2001).

Microinjections and molecular analysis

Morpholino oligonucleotides were diluted in 100 mM KCl and 10 mM HEPES and injections were performed using a nanoliter2000 microinjector (World Precision Instruments). Injection concentrations ranged from 0.05 mM to 0.2 mM and injection volume was set at 4.6 nl/embryo (1.4-7.4 ng/embryo). Efficiency of morpholino splicing was confirmed by RT-PCR. Total RNA from single embryos at different stages was isolated using Trizol according to the manufacturer's instructions. RT followed by nested PCR was performed with gene-specific nested forward and reverse primers, and purified for sequencing. Full-length mRNAs were injected into one- to two-cell embryos and grown at 28°C for further analysis.

Whole-mount in situ hybridization and immunohistochemistry

Whole-mount in situ hybridization on embryos of different stages was performed using antisense RNA probes labeled with digoxigenin or fluorescein (Boehringer Mannheim, Germany) as described previously (Thisse et al., 2004). Stained embryos were fixed, cleared with dimethylformamide, transferred into PBS:Glycerol (1:1) and photographed on a Leitz MZ12 or Nikon E800 microscope equipped with Spot Image digital camera. Whole-mount immunohistochemistry for NaK ATPase (alpha6F monoclonal) was performed as described by Drummond et al. (Drummond et al., 1998). Whole-mount double fluorescent in situ hybridization was performed as described previously [S. Holley, Yale University, CT, personal communication (Julich et al., 2005; Liu et al., 2007)]. Stained embryos were dehydrated in methanol, cleared with 2:1 benzyl benzoate:benzyl alcohol, and examined with a Zeiss LSM5 Pascal-confocal microscope. For in situ hybridization of sections, embryos were sectioned in JB-4 to a thickness of 10 μm and examined using a Nikon E800 microscope.

Histochemistry

Embryos for histological analysis were fixed with 4% paraformaldehyde (PFA) in PBS overnight, followed by dehydration and embedding in JB-4 (Polysciences) and sectioned at 5-7 μm. Slides were stained in Methylene Blue/Azure II (Humphrey and Pittman, 1974).

Acridine Orange and TUNEL staining

Apoptosis in the embryos was assessed by Acridine Orange and TUNEL (terminal transferase mediated dUTP nick end-labeling). Live embryos were used for apoptotic cell staining with the vital dye Acridine Orange as described (Barrallo-Gimeno et al., 2004). Embryos were incubated in the dark in a 5 μg/ml Acridine Orange solution (diluted from a 5 mg/ml stock) for 30 minutes, washed with egg water and analyzed under a fluorescent Nikon E800 microscope. TUNEL staining was performed on embryos fixed with 4% PFA-PBS overnight at 4°C as described (Chi et al., 2003). The fixed embryos were dechorionated, washed and transferred through a graded series of methanol:PBT to 100% methanol. The embryos were rehydrated and permeabilized by proteinase K, re-fixed in 4% PFA-PBS, washed with PBT and incubated in blocking solution (3% H_2O_2 in methanol) for 1 hour at room temperature. The embryos were then washed in PBT and incubated in permeabilization solution (0.1% Triton X-100 in 0.1% sodium citrate) for 5 minutes on ice. The permeabilized embryos were then incubated for 1-3 hours with terminal transferase (Roche) and fluorescein-labeled ddUTP at 37°C. The embryos were washed with PBT several times, incubated in converter POD for 30 minutes at 37ºC and detected using DAB.

Microangiography and vascular cell counts

48 hpf embryos were anaesthetized with Tricaine (16 mg/100 ml egg water), mounted in 3% methylcellulose and injected with a 5% solution of 2,000,000 Dalton Rhodamine dextran in Hank's buffer into the sinus venosus. After 5 minutes, the injected embryos were imaged on a Zeiss LSM5 Pascal confocal microscope. To quantify vascular cell number, nuclei were visualized in 15 μm plastic sections by DAPI staining. Endothelial cell nuclei were identified by tissue morphology using DIC optics to identify the cardinal vein and aorta in trunk cross-sections.

RESULTS

osr1 expression during gastrulation and somitogenesis

osr1 is expressed the germ ring at 30% epiboly (Fig. 1A) (Tena et al., 2007) and, at 75% epiboly, in cells dispersed over the yolk in a pattern similar to endoderm progenitors (Kikuchi et al., 2000). Two-color in situ hybridization using *osr1* and *no tail* (*ntl*) probes revealed that *osr1* expression is restricted to vegetal tiers of mesendodermal cells closest to the margin and is not present in more-animal cells that express *ntl*. *osr1* expression overlapped with *sox32* expression in the most vegetal tiers of germ ring mesendoderm but not in cells of the yolk syncytial layer (YSL) (Fig. 1E,F). To discern whether *osr1* was expressed in both mesoderm and endoderm progenitors, we used double-fluorescent in situ hybridization and confocal microscopy. Double-fluorescent in situ with *osr1* and *ntl* probes reveal that *osr1* and *ntl* expression overlapped in a subset of cells at 60% epiboly, whereas other more dispersed cells were positive for *osr1* but not for *ntl* (Fig. 1G-I). To determine whether these cells were endodermal

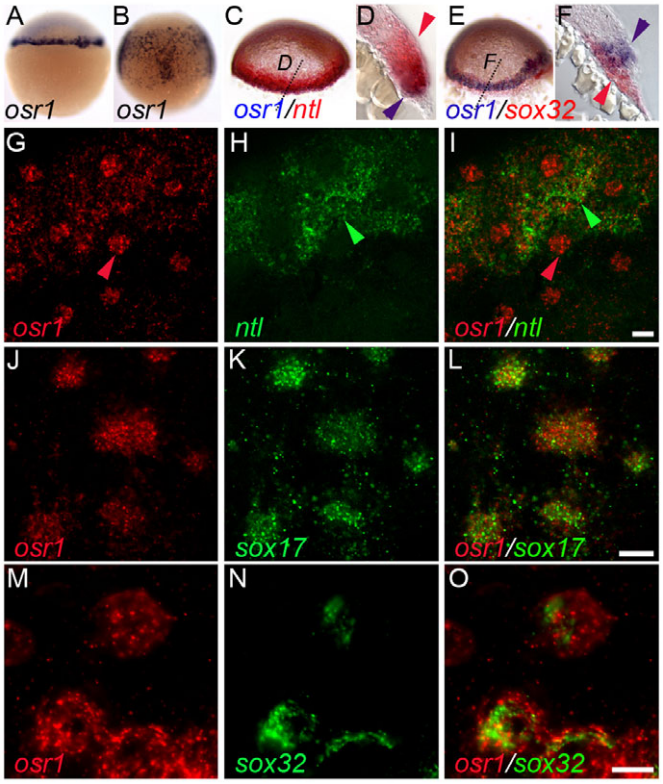

Fig. 1. *osr1* expression during early gastrulation. (**A**,**B**) *osr1* expression in the germ ring at 30% epiboly (A) and in the gastrulating cells at 75% epiboly (B). (**C**) Two-color in situ of *osr1* (blue) and *ntl* (red) mRNA transcripts at 30% epiboly. (**D**) Cross-section of C at the level indicated shows that *osr1* is not expressed in the *ntl*-positive mesodermal cells farther from the margin (red arrowhead) and is restricted to mesendoderm cells closest to the margin (blue arrowhead). (**E**) Colocalization of *osr1* (blue) and *sox32* (red) mRNA transcripts at 30% epiboly. (**F**) Cross-section of E at the level indicated shows *osr1* expression in the mesendoderm cells with some overlap with *sox32*-positive endodermal cells (blue arrowhead) but the absence of *osr1* expression in the *sox32*-positive YSL cells (red arrowhead). (G-O) Magnified lateral views of 60% epiboly embryos just above the blastoderm margin with dorsal on the right. (**G-I**) Double-fluorescent in situ hybridization of *osr1* (red) and *ntl* (green) probes at 60% epiboly. The images represent a maximum intensity projection of a confocal *z*-series stack (four slices, 1.9 μm each). (I) Merge of G and H showing distinct expression of *osr1* (G) in endoderm cells (red arrowhead, G,I) that do not express *ntl* (H). *osr1* (G) is co-expressed with *ntl* (H) in mesendoderm cells (green arrowhead, H,I). (**J-L**) Double-fluorescent in situ hybridization of *osr1* (red) and *sox17* (green) at 60% epiboly. Images represent a single confocal slice of 1.9 μm. (L) Merge of J and L showing co-expression of *osr1* and *sox17* in endoderm cells. (**M-O**) Double-fluorescent in situ hybridization of *osr1* (red) and *sox32* (green) at 60% epiboly. Images represent a single confocal slice of 1.9 μm. (O) Merge of M and N showing co-expression of *osr1* and *sox32* in endoderm cells. Scale bars: in G,I,L, 10 μm for G-O.

progenitors, we assayed expression of the endodermal markers *sox17* and *sox32*. Double-fluorescent in situ revealed that dispersed *osr1*-expressing cells also expressed *sox17* (Fig. 1J-L) and *sox32* (Fig. 1M-O). The data indicate that *osr1* is expressed in mesendoderm closest to the YSL at 30% epiboly; later, as epiboly progresses, *osr1* is expressed in endoderm progenitors as well as in mesodermal cells that express *ntl*.

Previous studies reported that zebrafish *osr1* was co-expressed with the nephric markers *pax2a* and *lim1* in the intermediate mesoderm during somitogenesis (Tena et al., 2007). To discern the *osr1* expression pattern at higher resolution, we assayed its expression relative to known IM/LPM markers using single and two-color in situ hybridization. At the tailbud stage (10 hpf), *lim1* is expressed in bilateral stripes of IM adjacent to presomitic mesoderm and in adaxial cells (Fig. 2A,B). By contrast, *osr1* was expressed in cells displaced laterally and ventrally from the *lim1* expression domain (Fig. 2C,D). During somitogenesis, this pattern persisted and *osr1* was detected in bands of cells that superficially appear to be the intermediate mesoderm; however, histological sections of 18 hpf embryos show that these *osr1*-expressing cells lie ventral and lateral to the pronephros, and are excluded from the forming pronephros (Fig. 2E,F). This is also clear at 24 hpf (Fig. 2G,H) where sections of the trunk show *osr1* expression in ventrolateral tissues, but not in the pronephros. Sections of 18 and 24 hpf embryos also revealed that *osr1* was expressed in the endoderm at the midline. Endoderm expression was confirmed by examining older embryos where *osr1* was shown to be expressed in the liver and gut at 48 hpf (see Fig. S1 in the supplementary material). Two color in situs revealed that *osr1*-expressing cells were lateral to *pax2a* (Fig. 2I,J), *scl* (Fig. 2L-M) and *etsrp1* (Fig. 2O-Q) expressing cells. Sections of embryos double-stained for *pax2a* and *osr1* confirmed that *osr1* is expressed ventrally and laterally to the forming kidney (Fig. 2K). We conclude that *osr1* is not expressed in the IM during somitogenesis, as previously reported. The lateral and ventral position of *osr1*-positive cells and the early expression *osr1* in both mesoderm and endoderm suggests that this tissue is likely to be the zebrafish equivalent of the splanchnopleure (Funayama et al., 1999). In light of previous reports on *osr1* function in nephrogenesis and our results that *osr1* is not expressed in kidney tissue, we re-examined the *osr1* loss-of-function phenotype.

osr1 is specifically required for proximal pronephric nephron development

Previous studies suggested that *osr1* loss of function resulted in the complete absence of kidney tissue and gross edema (Tena et al., 2007). By contrast, we found that *osr1* loss of function by morpholino knockdown (Fig. 3A,B) resulted in a segment-specific defect in the proximal nephron, whereas the distal nephron was relatively unaffected (Fig. 3C-F). The chloride-bicarbonate exchanger *ae2* is expressed highly in the proximal nephron and at a lower level in the distal nephron at 24 hpf (Fig. 3C) (Shmukler et al., 2005). In *osr1* morphants, *ae2* expression is specifically missing in the proximal nephron, whereas expression in the distal nephron is unchanged (Fig. 3D; 90% of injected embryos; n=10). Expression of the NaK ATPase α subunit marks the full length of the nephron at 72 hpf (Drummond et al., 1998) (Fig. 3E). In confocal images of *osr1* morphants, NaK ATPase-positive tubules were truncated, with proximal tubule segments missing (100% of injected embryos, n=15; Fig. 3F). Both NaK ATPase staining and *ae2* in situ often revealed an asymmetric loss of the proximal nephron (Fig. 3D). In one experiment, nine out of 17 embryos showed asymmetric loss of the proximal nephron, while the remaining eight showed a symmetric loss (as shown in Fig. 4H). Similar proximal segment-specific loss was observed using in situ probes for *lim1*, *pax8*, *osr2* and *nbc1* (data not shown). Expression of more distal nephron segment markers *trpM7* (Elizondo et al., 2005; Liu et al., 2007; Wingert et al., 2007) and *ret1* (Bisgrove et al., 1997; Marcos-Gutierrez et al., 1997) were unaffected by *osr1* loss of function (see Fig. S2 in the supplementary material). Similar results were obtained with both an *osr1* ATG

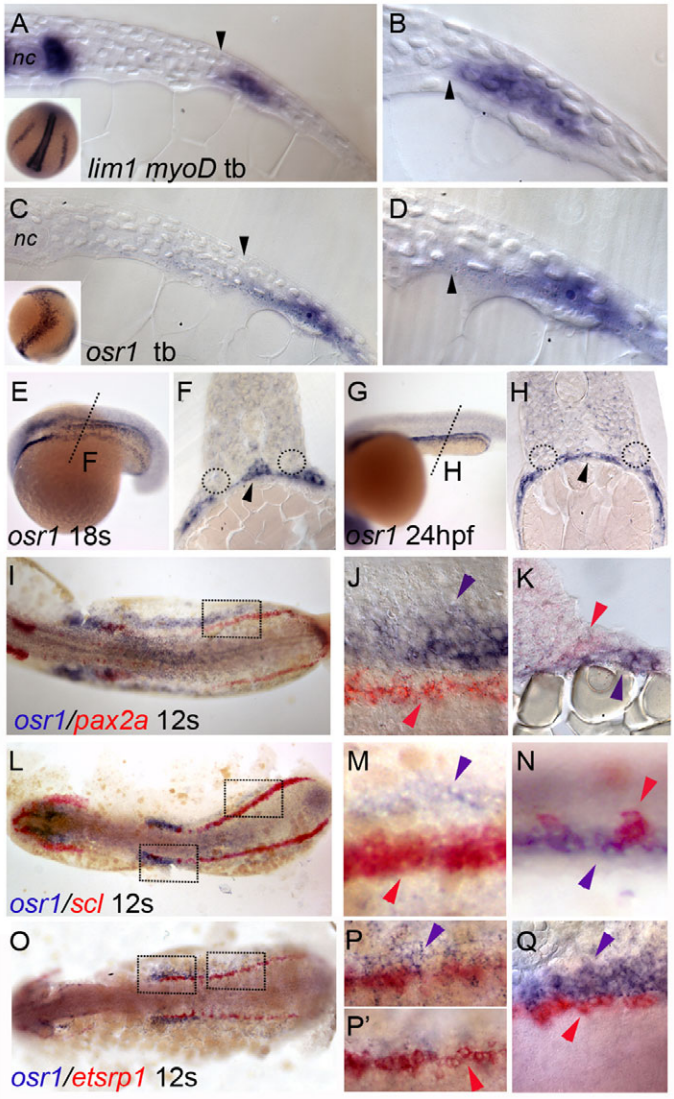

Fig. 2. *osr1* expression during zebrafish development. (**A**) Cross-section of a tailbud stage embryo showing expression of *lim1* in cells of the IM (A, inset) adjacent to presomitic mesoderm (arrowhead) and *myoD* in adaxial cells adjacent to the notochord (nc). (**B**) Magnification of A showing proximity of *lim1*-positive IM to the border of presomitic mesoderm (arrowhead). (**C**,**D**) Cross-section of a tailbud stage embryo showing expression of *osr1* in bilateral stripes (inset, C) in cells lateral and ventral to the expression of *lim1* (C,D) (arrowheads indicate the anatomical border of presomitic mesoderm. (**E**) At 18 somites, *osr1* is expressed in bilateral stripes just anterior to the somites and in lateral mesoderm of the trunk and tail. (**F**) Cross-section of embryo in E at the level indicated in E showing *osr1* expression ventral and lateral to the pronephros (outlined in F) and endodermal cells (arrowhead, F). (**G**) *osr1* expression at 24 hpf in cells overlying the yolk extension. (**H**) Cross-section of the embryo in G at the level indicated shows *osr1* expression in the ventrolateral mesoderm distinct from the pronephric ducts (circles) and in endoderm (arrowhead, H). (**I-K**) Expression of *osr1* (blue) and *pax2a* (red). (J) Magnified views of boxed region in I show non-overlapping expression of *osr1* (blue arrowhead) and *pax2a* (red arrowhead) in the intermediate mesoderm. (K) Cross-section at the same level shows expression of *osr1* (blue arrowhead) in cells ventral and lateral to the cells expressing *pax2a* (red arrowhead). (**L-N**) Expression of *osr1* (blue) and *scl* (red) at 12 somites. Magnified views of boxed regions in L show non-overlapping expression of *osr1* and *scl* in the posterior (M) and anterior (N) regions of the PLM. (**O-Q**) Expression of *osr1* (blue) and *etsrp1* (red) at 12 somites. Magnified views of boxed regions in O show non-overlapping expression of *osr1* and *etsrp1* in the posterior (P,P′) and anterior (Q) regions of the PLM. (P,P′) Magnified view of the boxed region in O at different focal planes showing *osr1*- and *etsrp1*-positive cells at different dorsoventral positions, with *osr1* in more ventral (P) and *etsrp1* in the more dorsal cells (P′) with reference to yolk cells.

initiation codon blocking morpholino and the exon 2 splice donor morpholino; all subsequent experiments were performed with the exon 2 donor morpholino as we could more rigorously determine the efficacy of *osr1* knockdown using RT-PCR. Apoptosis assays also revealed that loss of the proximal nephron was not due to cell death (see Fig. S3 in the supplementary material). These results indicate that kidney defects in *osr1* morphants are specific to the proximal nephron and also that *osr1* loss of function does not result in a general re-patterning of nephron segments.

osr1 is required for glomerular morphogenesis

To determine whether pronephric glomerular development was affected by *osr1* knockdown, we assayed expression of the Wilms tumor suppressor gene *wt1a*, a marker of podocyte specification (Bollig et al., 2006; Drummond et al., 1998; Majumdar and Drummond, 1999; Perner et al., 2007; Serluca and Fishman, 2001). In wild-type embryos, *wt1a* is expressed in anterior lateral mesoderm (Serluca and Fishman, 2001) and strongly in prospective pronephric podocytes at 24 hpf (Fig. 4A,C). At 48 hpf, *wt1a*-positive podocytes surround a compact glomerular vascular tuft derived from the aorta (Fig. 4E) (Drummond et al., 1998; Majumdar and Drummond, 1999). In *osr1* morphants, *wt1a* was expressed at 26 hpf, although in a somewhat more dispersed pattern (Fig. 4B). Histological sections showed bilateral groups of podocyte progenitors ventral to the somites in all *osr1* morphant embryos (Fig. 4D). However, these progenitors failed to coalesce into a compact structure at the midline, and a mature vascularized glomerulus is never formed. *nephrin* is an essential component of the pronephric glomerulus and is expressed in podocytes in wild-type embryos (Fig. 4G) (Kramer-Zucker et al., 2005). *osr1* loss of function eliminated *nephrin* expression in podocytes (91% of injected embryos, n=12; Fig. 4H). Similarly, expression of *podocin*, another podocyte-specific marker, was absent from the glomerulus in *osr1* morphants (data not shown). The data suggest that *osr1* is not required for podocyte specification but rather functions at a later step in glomerular maturation associated with integration of blood vessels with podoctyes and the expression of the podocyte cell adhesion molecules *nephrin* and *podocin*.

osr1 loss of function expands the angioblast cell lineage

As derivatives of the IM/LPM also include the vasculature, blood and the heart, we analyzed the expression of vascular and blood markers in wild-type and *osr1* morphant embryos. The transcription factor *scl* is expressed in both vascular and hematopoietic progenitor cells (Gering et al., 1998). In zebrafish, *scl* is first expressed during somitogenesis in cells that occupy bilateral stripes in the trunk IM/LPM (Gering et al., 1998) (Fig. 5A,C). Strikingly, the number of *scl*-expressing cells in the IM/LPM was significantly expanded in *osr1* morphants at the 12-somite stage (89% of injected embryos,

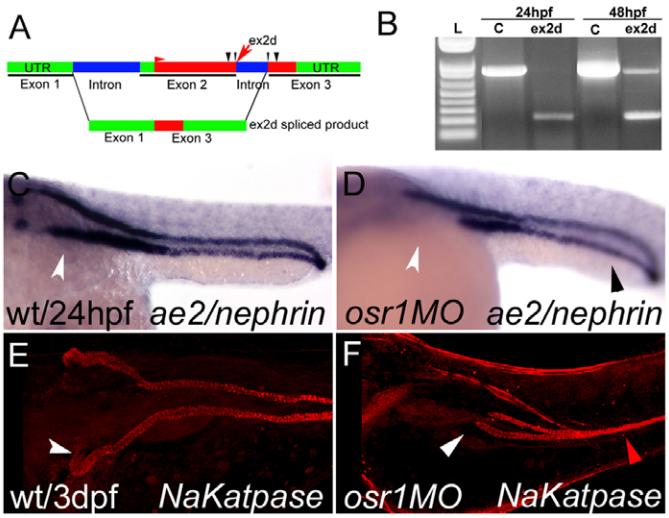

Fig. 3. *osr1* knockdown results in segment-specific kidney defects. (**A**) *osr1* gene structure and morpholino oligo targeting exon 2 (ex2d). (**B**) RT-PCR analysis of morpholino-induced *osr1* mis-splicing. Blocking the exon 2 splice donor sequence resulted in the complete deletion of exon 2, which contains the ATG start codon and the entire coding sequence for the *osr1* transcriptional regulatory domain and the first zinc finger. In embryos injected with 7.4 ng morpholino, no wild-type mRNA was detectable at 24 hpf, indicating that these morphant embryos were functionally null for *osr1*. A five-base pair mismatch control morpholino did not cause any molecular or phenotypic defects. Co-injection of *osr1* synthetic mRNA along with the exon 2 donor morpholino rescued the *osr1* phenotype in 53% (9/17) of embryos, as determined by *pax2a* expression (see Results), demonstrating specificity of the morpholino knockdown. (**C**) Expression of *ae2* in the proximal pronephros (white arrowhead) is absent in *osr1* morphants (**D**), whereas the distal pronephros is unaffected (black arrowhead). Immunofluorescence using anti-NaK ATPase alpha6F monoclonal antibody labels the entire pronephros in wild-type embryos (**E**), whereas expression is specifically lost (**F**) in the proximal nephron (white arrowhead) of *osr1* morphants, leaving the distal pronephros unaffected (red arrowhead).

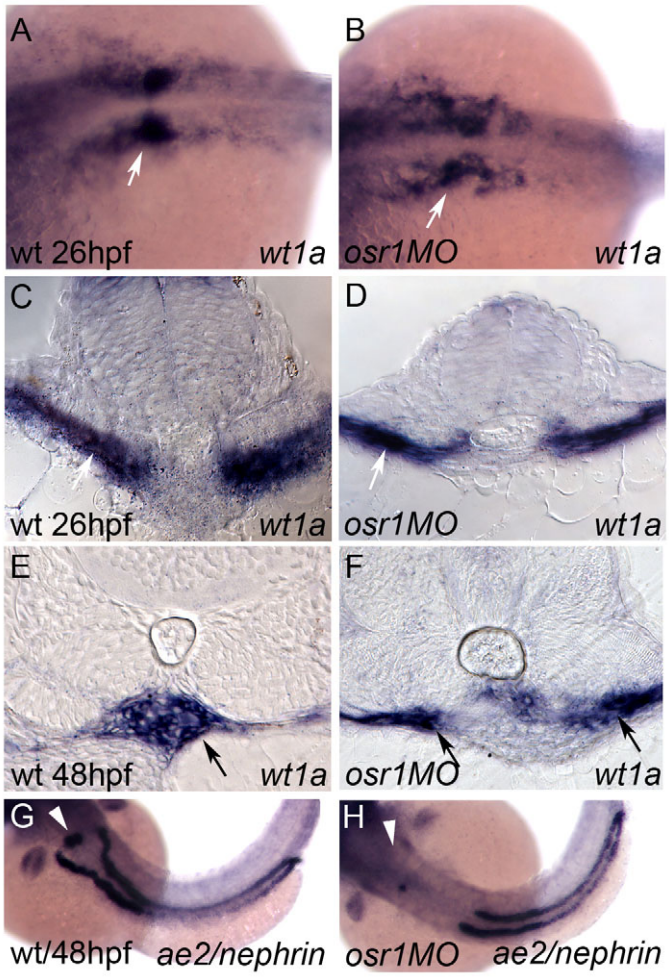

Fig. 4. *osr1* is required for glomerular morphogenesis. (**A**,**B**) Expression of *wt1a* in control (A) and *osr1* morphants (B) at 26 hpf. (**C**,**D**) Histological cross-sections of the 26 hpf glomerular progenitors in wild-type (C) and *osr1* morphants (D) show equivalent expression of *wt1a* (arrows). (**E**,**F**) Cross-section of wild-type glomerulus at 48 hpf (E) shows *wt1a* expression in the midline vascularized glomerulus (arrow), whereas in *osr1* morphants (F) *wt1a*-positive podocytes remain in an immature state (arrows) and fail to coalesce to the midline. (**G**,**H**) Expression of the podocyte marker *nephrin* is lost in *osr1* morphants (arrowhead, H) when compared with the control embryos (arrowhead, G). Segment-specific loss of *ae2* expression in the proximal pronephros is evident in the *osr1* morphants (H) when compared with controls (G) at 48 hpf.

n=19; arrows, Fig. 5B). This expansion was most obvious in the anterior IM/LPM adjacent to somites 1-8 and to the domain of proximal nephron *pax2a* expression in wild-type embryos (Fig. 5A). Embryo staging was confirmed by double color in situ with *myoD* and *scl* (see Fig. S4 in the supplementary material). Expanded *scl* expression could also be seen in the posterior IM at 12 somites (Fig. 5D) and was evident in the region of the forming venous plexus at 26 hpf (100% of injected embryos, *n*=17; Fig. 5G,H). As *scl*-expressing cells could represent progenitors of either vascular or hematopoietic lineages (Gering et al., 1998), we next asked whether a specific lineage was affected by loss of *osr1*. *flk1*, the endothelial cell-specific receptor for VEGF is initially expressed in hemangioblasts and subsequently maintained in endothelial cells during vessel formation (Habeck et al., 2002; Liao et al., 1997; Thompson et al., 1998). Similar to *scl*, *flk1* is expressed during early somitogenesis in bilateral stripes of IM/LPM cells (Liao et al., 1997) (Fig. 5C) that subsequently contribute to the main trunk vessels (Liao et al., 1997). In 12-somite *osr1* morphants, expression of *flk1* is significantly upregulated in the anterior trunk, similar to what we observed for *scl* expression (86% of injected embryos, *n*=35; arrows, Fig. 5D). *etsrp1* is the earliest expressed transcription factor that controls vascular development without affecting hematopoietic development (Sumanas and Lin, 2006). Similar to *scl* and *flk1*, *etsrp1* is expressed in bilateral stripes in the head and trunk of wild-type embryos during somitogenesis (Sumanas and Lin, 2006) (Fig. 5E). In 12-somite *osr1* morphants, *etsrp1*e-epressing cells are significantly expanded in the anterior trunk IM/LPM (90% of injected embryos, *n*=11; arrows, Fig. 5F).

The effect of *osr1* on hematopoietic lineages was evaluated with the markers *pu.1* for the monocytic lineage (Lieschke et al., 2002) and *gata1* for the erythropoietic lineage (Detrich et al., 1995). In wild-type embryos, *pu.1*-positive myeloid progenitors are expressed in both the rostral blood island and the posterior intermediate mesoderm or caudal blood island (Fig. 5I). Contrary to what we observe for *scl*, *flk* and *etsrp*, in *osr1* morphants, *pu.1* expression was not expanded and in fact was reduced in the anterior IM/LPM (87%

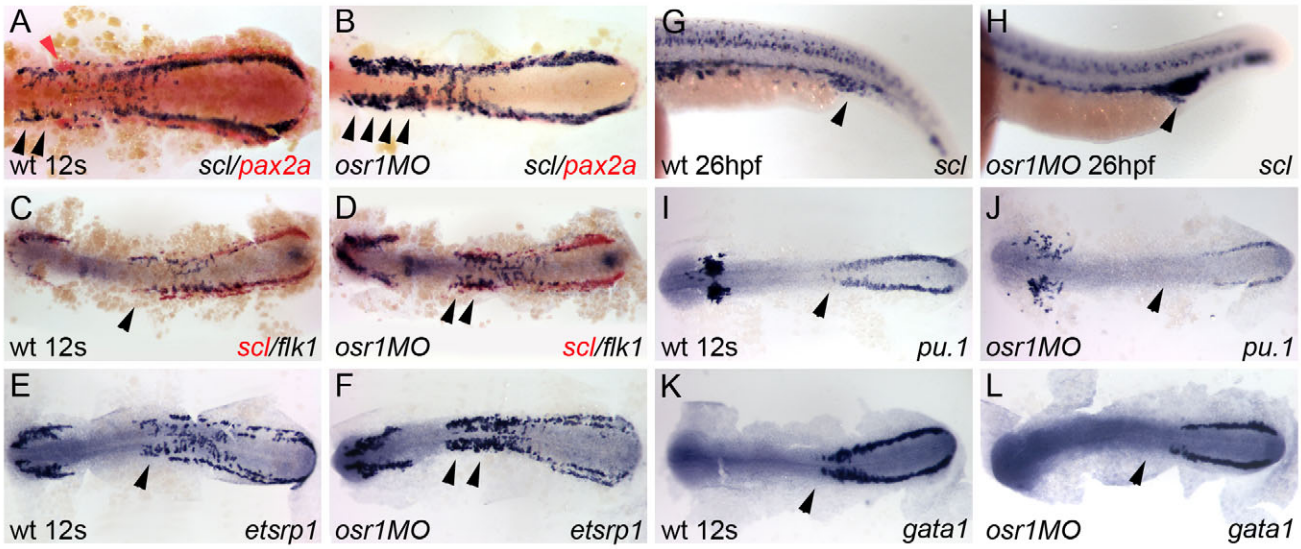

Fig. 5. *osr1* knockdown expands vascular progenitor tissue. (**A**) *scl* (blue) and *pax2a* (red) expression in wild-type embryos labels adjacent bands (arrowheads) of intermediate mesoderm in 12-somite stage wild-type embryos. (**B**) *osr1* knockdown results in expansion of *scl*-positive tissue, most prominently in anterior LPM (arrowheads) and loss of *pax2a*-expressing cells. (**C**) *flk1* (blue) and *scl* (red) expression in 12-somite wild-type embryos (arrowhead). (**D**) *osr1* knockdown increases the number of *flk1*-expressing cells (arrowheads). (**E**) *etsrp1* expression in control 12-somite embryos (arrowhead). (**F**) *etsrp1* expression is expanded in 12-somite stage *osr1* morphants (arrowheads). (**G**) At 26 hpf, *scl* is expressed in the blood islands and forming venous plexus (arrowhead). (**H**) 26 hpf *osr1* morphants show an expansion of *scl*-positive tissue in the region of the forming venous plexus (arrowhead). (**I**,**J**) Expression of the monocyte lineage marker *pu.1* in wild-type embryos (I) and *osr1* morphants (J) shows a reduction of expression in the anterior aspect of its LPM expression domain (arrowheads). (**K**,**L**) Similarly, expression of the erythrocyte marker *gata1* in wild-type embryos (K) and *osr1* morphants (L) shows a reduction of expression in its most anterior expression domain (arrowheads).

of injected embryos, *n*=16; Fig. 5J). We also found that migration of *pu.1*-expressing ALM macrophages appears advanced compared with controls (Fig. 5J). Similarly, expression of *gata1*-positive erythrocyte progenitors (Fig. 4K) was not expanded (arrow, Fig. 5L) and in fact was reduced in the anterior IM/LPM (74% of injected embryos, *n*=35). Analysis of the cardiac-specific homeobox gene *nkx2.5* (Chen and Fishman, 1996) showed normal expression in *osr1* morphants, indicating that *osr1* does not affect the specification of cardiac progenitors (data not shown). These results indicate that *osr1* is not only required for proximal nephron development but also acts to limit angioblast cell differentiation, most notably in the anterior IM/LPM.

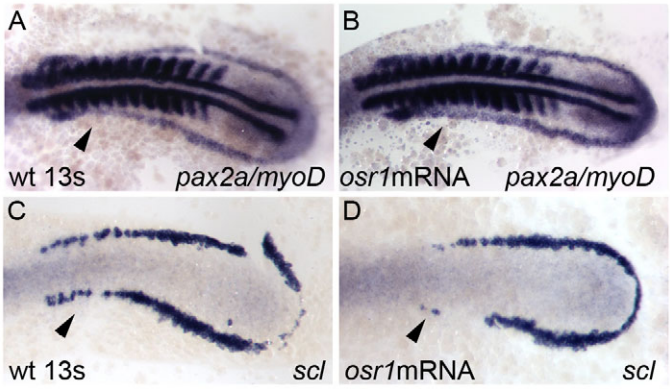

Fig. 6. Overexpression of *osr1* causes expansion of pronephric progenitor number and a reduction in angioblast number. Control embryos (A,C) and embryos injected with 100 pg of *osr1* mRNA (B,D). (**A**) Control expression of *pax2a* is expanded after injection of *osr1* mRNA (**B**), specifically in the mid-portion of the IM (arrowhead, B), which is normally downregulated in the control embryos at the 13-somite stage (arrowhead, A). *myoD* is used as an internal control for somite staging in these embryos (A,B). (**C**,**D**) Expression of *scl* is lost in the anterior lateral plate mesoderm (arrowhead, D) in the embryos injected with *osr1* mRNA when compared with the uninjected controls (arrowhead, C).

osr1 overexpression expands kidney progenitors at the expense of angioblast cell number

To confirm results on *osr1* loss of function, we tested whether *osr1* gain of function would have opposite effects on patterning the anterior IM/LPM. By the 13-somite stage, *pax2a* is normally downregulated in the mid-portion of the IM in wild-type embryos (Fig. 6A). Ectopic expression of *osr1* by synthetic *osr1* mRNA injection at the one-cell stage resulted in enhanced expression of *pax2a* throughout the IM and specifically prevented the downregulation of *pax2a* in the mid-portion of the IM (78% of injected embryos, *n*=32; Fig. 6B). In a complementary fashion, *scl* expression in the anterior LPM (Fig. 6C) was specifically lost in *osr1* morphants (70% of injected embryos, *n*=27) (Fig. 6D). No ectopic expression of either lineage marker was induced outside of their respective expression domains by *osr1* overexpression. The results indicate that overexpression of *osr1* is sufficient to re-pattern the anterior IM/LPM, adjacent to somites 1-8.

osr1 is required for pronephric epithelial differentiation and to limit the size of the axial vein

To assess whether a re-specification of mesoderm occurs in *osr1* morphants, we sectioned control (Fig. 7A) and *osr1* morphants (Fig. 7B) at 52 hpf, prior to the development of gross edema, to

examine the morphology of the glomerulus, pronephric ducts and vasculature. At the level of pectoral fin in control embryos (Fig. 7C, inset), the glomerulus was visible ventral to the aorta as a compact structure (arrowhead, Fig. 7C). However, in *osr1* morphants, all sectioned embryos lacked a vascularized glomerulus and pronephric tubules at the level of the pectoral fin (Fig. 7D, inset; *n*=4). Instead, all sectioned embryos showed prominent profiles of the cardinal veins (Fig. 7D, *n*=4), which in serial sections, could be distinguished from the pronephros by the presence of red blood cells in the lumen. In more posterior sections of wild-type embryos (Fig. 7E), the pronephros was visible as bilateral epithelial tubules (arrowhead, Fig. 7E) that flank the medial aorta and vein, here filled with nucleated red blood cells. In *osr1* morphants, the pronephric tubules in the trunk were present but appeared smaller (arrowhead, Fig. 7F) compared with controls.

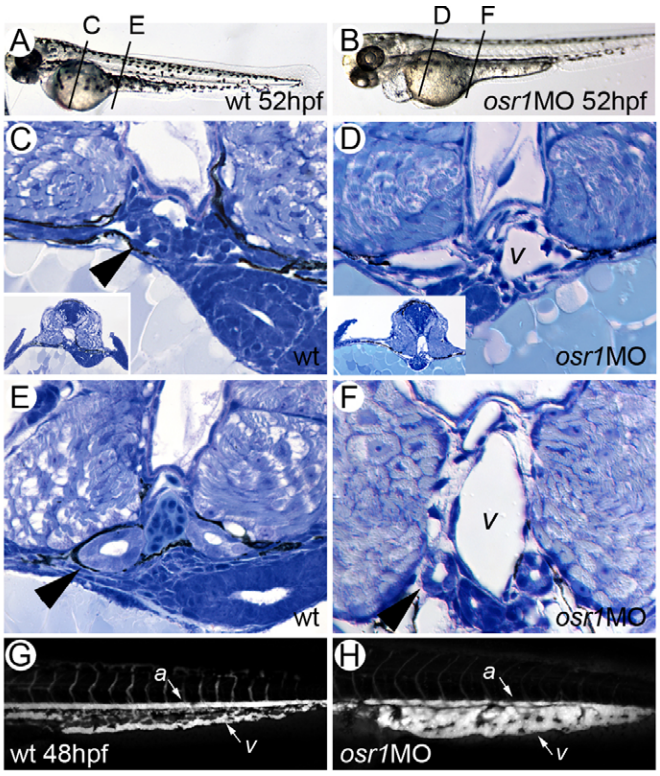

Fig. 7. Loss of pronephric epithelial differentiation and vascular expansion in *osr1* morphants. Control (A,C,E,G) and *osr1* morphants (B,D,F,H) at 52 hpf. (**A**) Wild-type 52 hpf embryo showing position of histological sections in C and E. (**B**) *osr1* morphant embryo showing position of histological sections in D and F. (**C**) Cross-section at the level of the fin buds (inset) shows normal glomerular structure (arrowhead) and connecting pronephric tubules. (**D**) Cross-section at the level of the fin buds in an *osr1* morphant (inset) shows absence of pronephric tubules and glomerulus and expansion of cardinal vein (*v*). (**E**) In more posterior sections of wild-type embryos, the pronephric epithelial tubules (arrowhead) and cardinal vein are of roughly similar dimensions. (**F**) In *osr1* morphants, pronephric tubules are reduced in diameter compared with wild-type (arrowhead) and the cardinal vein (*v*) is significantly expanded. (**G**) Angiogram of wild-type embryo trunk and tail region highlights the aorta (*a*) and the common tail vein (*v*). (**H**) Angiogram of an *osr1* morphant highlights a grossly expanded venous plexus in the tail (*v*). Intersomitic vessels were present in *osr1* morphants but are not shown in the confocal sections used in this projection.

Strikingly, the size of the medial vein was significantly enlarged in *osr1* morphants (*v* in Fig. 7F) at all the A-P levels examined (*v* in Fig. 7D,F). To determine whether the increase in vein lumen size was associated with a corresponding increase in vein endothelial cell number and to rule out the possibility that vein expansion was secondary to edema, we counted DAPI stained endothelial cell nuclei in 15 μm sections (from the trunk region, as in Fig. 7E,F) of 36 hpf *osr1* morphants that showed no pericardial expansion or other evidence of edema. *osr1* morphants showed a significant increase in the number of vein endothelial cell nuclei [5.11±0.19/section (s.e.m.), *n*=26 compared with 3.04±0.09/section, *n*=25 in control]. Arterial size and endothelial cell number were not affected (2.6±0.1, *n*=25 in control versus 2.8±0.14, *n*=26 in morphants) in *osr1* morphants. To further analyze the enlargement of veins in *osr1* morphants, we performed microangiography on control and *osr1* morphants at 48 hpf. Control embryos and *osr1* morphants showed normal circulation in the dorsal aorta and intersomitic vessels. However, the venous plexus region distal to the yolk extension was dramatically expanded in all *osr1* morphants examined (*v* in Fig. 7H; *n*=5) when compared with the control embryos (*v* in Fig. 7G). Taken together, the histology, cell counting and microangiography data strongly suggest that the venous cell fate is expanded in *osr1* morphants.

osr1 acts upstream of *pax2a* in kidney development

Pax2 and Pax8 are known to function partially redundantly to control kidney development in the mouse (Bouchard et al., 2002). In zebrafish, *pax2a* is specifically required for proximal tubule cell differentiation in the pronephros (Majumdar et al., 2000). We therefore tested whether ectopic expression of *pax2a* in *osr1* morphants would be sufficient to bypass a requirement for *osr1* and revert the *osr1* morphant phenotype to wild-type patterning of kidney and vascular tissues. We used the expression of *ae2* as a measure of the proximal nephron length in control and experimental embryos. The length of *ae2*-positive proximal tubules in control embryos ranged from 300-500 μm (mean of 378 μm; 14/14, 100%) (Fig. 8A,G). In *osr1* morphants, *ae2* segment length was reduced (Fig. 8B) with 42% of embryos (11/26) in the 100-200 μm range, 50% of embryos in the 200-300 μm range and only 8% of the embryos (2/26) exhibiting wild-type segment length (Fig. 8G). The overall mean *ae2*-positive tubule length for *osr1* morphants was 214 μm compared with 378 μm for controls. Injection of *pax2a* mRNA into *osr1* morphants restored 60% of the embryos (18/28) to the wild-type proximal tubule length of 300-500 μm (mean of 331 μm) (Fig. 8C). In a complementary fashion, *pax2a* expression reverted the expanded domain of *scl* expression (compare Fig. 8D with 8E) to a wild-type pattern (Fig. 8F). The data indicate that in the absence of *osr1* function, ectopic expression of *pax2a* is sufficient to specify proximal pronephric tubule differentiation. In addition, ectopic expression of *pax2a* is sufficient to limit angioblast differentiation in the intermediate mesoderm.

osr1 effects on mesoderm patterning are mediated by the endoderm

The simplest interpretation of our results so far would be that *osr1* functions early in the IM/LPM upstream of *pax2a* and *scl* to drive kidney development while repressing angioblast differentiation. However, several inconsistencies with this model were evident in our data. First, our finding that the anterior IM/LPM was preferentially affected in *osr1* morphants was not consistent with the broad posterior expression of *osr1* in the IM that extended to the

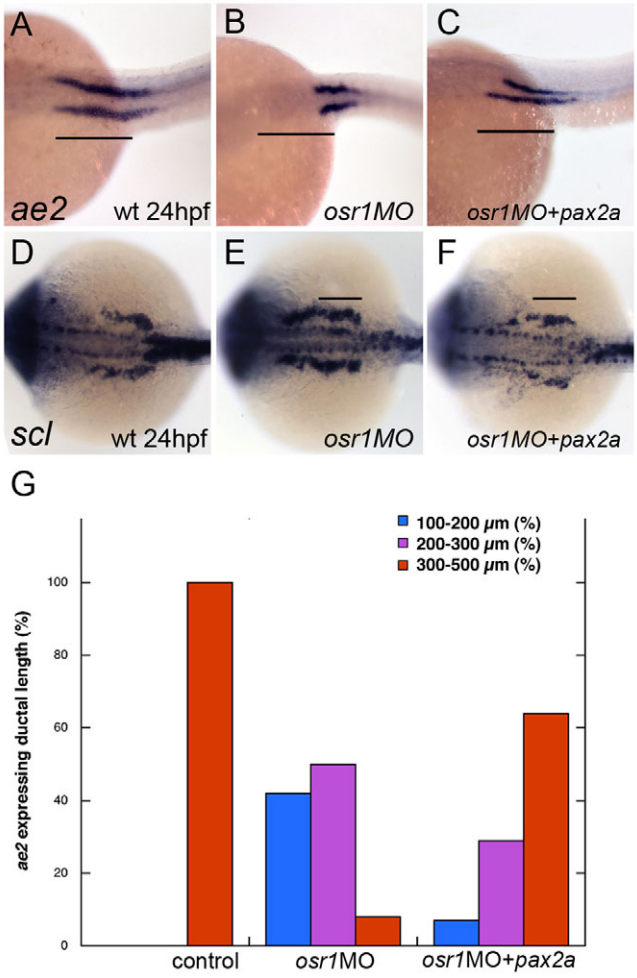

Fig. 8. Ectopic expression of *pax2a* rescues intermediate mesoderm patterning in *osr1* morphants. (**A-C**) Expression of *ae2* in the pronephros of 24 hpf control (A), *osr1* morphant (B) and *osr1* morphant co-injected with *pax2a* mRNA (C). Horizontal lines indicate the length of the wild-type *ae2*-positive proximal nephron segment. (**D-F**) Expression of *scl* in the anterior lateral mesoderm of 24 hpf control (D), *osr1* morphant (E) and *osr1* morphant co-injected with *pax2a* mRNA (F). Horizontal lines indicate the length of the wild-type *scl*-positive anterior lateral mesoderm. (**G**) Quantification of *pax2a* rescue of *ae2*-positive proximal pronephric nephron cells (see text for details).

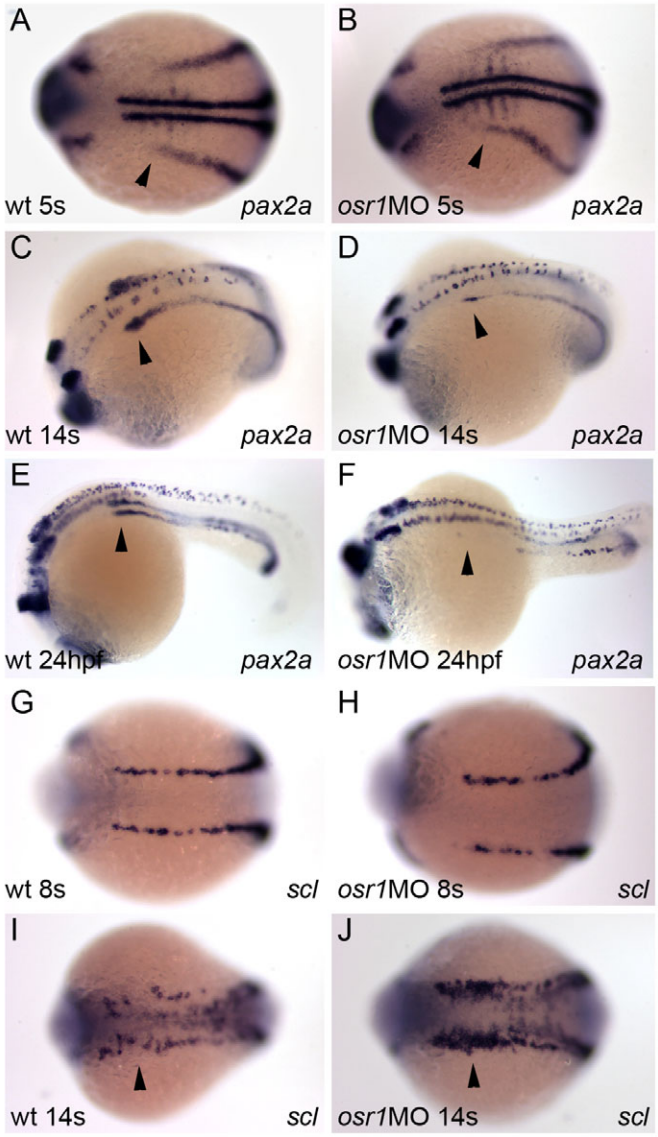

Fig. 9. *osr1* knockdown does not affect specification of pronephric and angioblast mesoderm, but does affect their subsequent maintenance. (**A**,**B**) Expression of *pax2a* and *myoD* in control (A) and *osr1* morphants (B) is similar at five somites (arrowheads in A and B). *myoD* is used as a internal somite staging control. (**C**,**D**) Expression of *pax2a* in a 14-somite control (C) and *osr1* morphants (D) reveals a substantial reduction in the number of *pax2a*-positive cells in the anterior IM (arrowheads, C,D). (**E**,**F**) Expression of *pax2a* in 24 hpf control (E) and *osr1* morphants (F) shows a complete loss of *pax2a*-positive cells in the proximal pronephros (arrowheads, E,F). (**G**,**H**) Expression of *scl* in *osr1* morphants (H) is similar to that of control embryos at 8 somites (G). (**I**,**J**) However, by the 14-somite stage, the number of *scl*-expressing cells is significantly upregulated in the anterior lateral plate mesoderm of *osr1* morphants (arrowhead, J) when compared with control embryos at the same stage (arrowhead, I).

tailbud (Fig. 2C, inset). We were also surprised to find that the re-patterning of the IM/LPM by *osr1* loss of function occurred progressively during somitogenesis and was not evident at the earliest stages of *pax2a* and *scl* expression. The early expression pattern of *pax2a* at the 5-somite stage in *osr1* morphants (Fig. 9B) was, in fact, similar to the wild-type pattern (Fig. 9A). However the anterior IM *pax2a* expression domain at the 14-somite stage (Fig. 9C) was reduced in *osr1* morphants (89% of injected embryos, n=37; Fig. 9D) and, by 24 hpf, completely absent (96% of injected embryos, n=53) (compare Fig. 9E with 9F). Similarly, *scl* expression was normal at the 8-somite stage in *osr1* morphants (Fig. 9G,H) and only later, at the 14-somite stage, was found to be expanded in *osr1* morphants (89% of injected embryos, n=19) (Fig. 9I,J). We could also rule out that the intermediate mesoderm was patterned by an antagonistic relationship between genes downstream of *osr1* (*pax2a* and *scl*) as loss of function in these genes alone, or in combination with *osr1* loss of function, did not result in expansion of the opposing lineage (see Fig. S5 in the supplementary material). These results, together with our finding that ectopic expression of *osr1* only affected cell differentiation within the anterior IM/LPM, suggested that *osr1* might act indirectly to pattern the mesoderm.

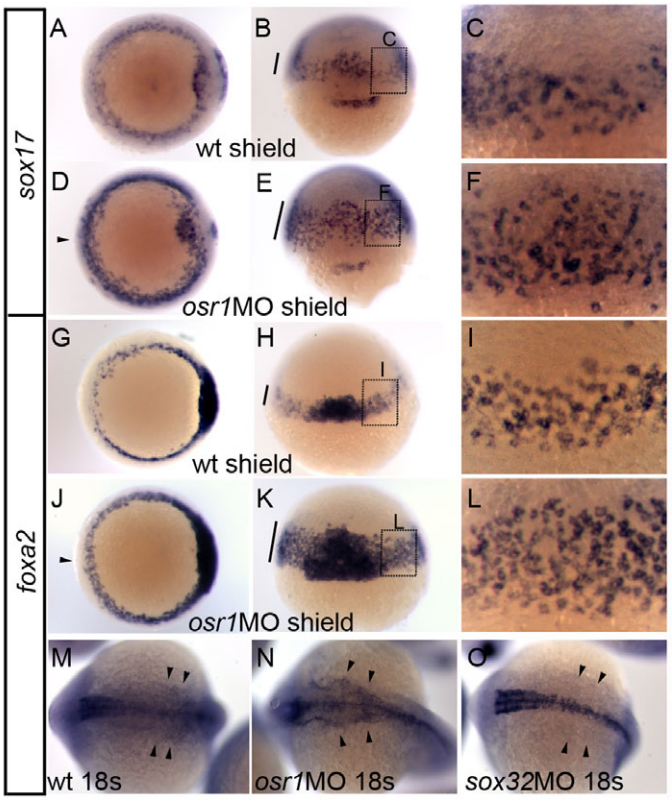

Fig. 10. *osr1* knockdown causes expansion of endoderm. (**A-F**) Expression of endoderm marker *sox17* in control (A-C) and *osr1* morphants (D-F) at the shield stage. (A,D) Dorsal views; (B,E) side views with dorsal facing; (C,F) magnified views of boxed regions in B,E, respectively. The number of tiers of *sox17*-expressing cells was significantly increased in *osr1* morphants at the blastoderm margin (bar in E,F) and in the ventral region of the embryo (arrowhead, D) when compared with control (A,C; bar in B). (**G-L**) Expression of mesendoderm marker, *foxa2* in control (G-I) and *osr1* morphants (J-L) at the shield stage. (G,J) Dorsal views; (H,K) side views with dorsal facing; (I,L) magnified views of boxed regions in H,K, respectively. The number of tiers of *foxa2*-expressing cells were significantly increased in *osr1* morphants with more layers of *foxa2*-expressing cells at the blastoderm margin (bar in K,L) and enhanced expression in the ventral region of the embryo (arrowhead, J) when compared with control (G,I; bar in H). (**M-O**) Expression of *foxa2* at 18 somites in control (M), *osr1* morphants (N) and *sox32* (*cas*) morphants (O). Development of *foxa2*-positive pharyngeal endoderm was enhanced in *osr1* morphants (arrowheads, N) when compared with control embryos (arrowheads, M) and was completely blocked by *sox32* knockdown (arrowheads, O).

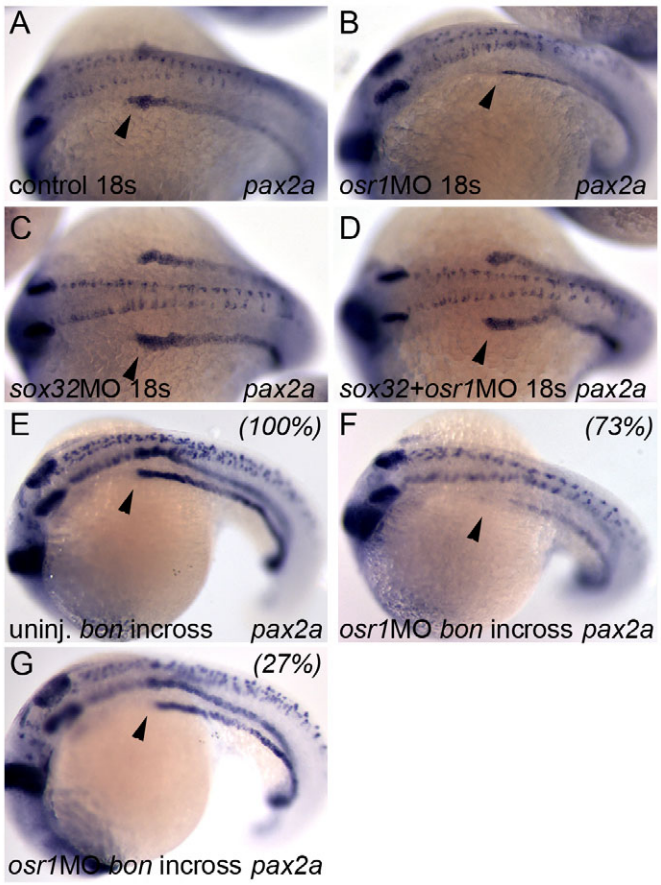

Fig. 11. Elimination of endoderm development in *osr1* morphants rescues proximal pronephric phenotype. (**A-D**) Expression of *pax2a* in control (A), *osr1* morphant (B), *sox32* morphant (C) and *osr1+sox32* double morphants (D). Loss of *osr1* resulted in loss of proximal *pax2a* pronephric expression (arrowhead, B) when compared with control 18-somite stage embryos (arrowhead, A). *sox32* (*cas*) morphants lacking endoderm showed slightly enhanced expression of *pax2a* in the proximal nephron (arrowhead, C). The loss of *pax2a* expression in the proximal pronephros of *osr1* morphants was rescued by elimination of endoderm in the *osr1+ sox32* double morphants (arrowhead, D). (**E-G**) Expression of *pax2a* in uninjected *bon* heterozygote incross embryos (E) and *osr1* morpholino injected *bon* incross embryos (F,G) at 24 hpf. *pax2a* expression was lost from the proximal pronephros in 47 out of 64 of the injected embryos (73%) (F). Loss of *pax2a* expression from the proximal pronephros was rescued in 17 out of 64 (27%) *osr1* MO injected, *bon* heterozygote incross embryos. Arrowheads in E-G indicate expression of *pax2a* in the proximal pronephros.

In addition to its expression in the IM/LPM, *osr1* is expressed in the germ ring mesendoderm at the shield stage (Fig. 1) (Tena et al., 2007). We examined whether *osr1* might function in mesendoderm patterning by assessing expression of the endoderm-specific markers, *foxa2* and *sox17*. Strikingly, we found that endoderm differentiation was strongly enhanced in *osr1* morphants. The number of *sox17*-positive cells at the shield stage (Fig. 10A-C) was significantly increased in *osr1* morphants (100% of injected embryos, *n*=14; Fig. 10D-F). Similarly, the number of *foxa2*-positive cells (Fig. 10G-I) was increased in *osr1* morphants (71% of injected embryos, *n*=21; Fig. 10J-L). Intensified expression of *foxa2* at the 18-somite stage (86% of injected embryos, *n*=15; Fig. 10M,N) confirmed that development of the pharyngeal endoderm was enhanced by *osr1* loss of function. *sox32*/*casanova* is a transcription factor that is required for all endodermal development (Alexander et al., 1999). As previously reported (Dickmeis et al., 2001), knockdown of *sox32* using an antisense morpholino (Dickmeis et al., 2001) specifically eliminated *foxa2*-expressing endoderm (93% of injected embryos, *n*=15) but did not affect *foxa2* expression in axial mesoderm (Fig. 10O).

The ability to block endoderm development by *sox32/casanova* knockdown allowed us to test whether expanded endoderm development was responsible for re-patterning the mesoderm in the context of *osr1* loss of function. As expected, knockdown of *osr1* alone resulted in a reduction in *pax2a*-positive cells (90% of injected embryos, *n*=43; Fig. 11B) compared with control (Fig. 11A) at 18

somites. Knockdown of *sox32* alone did not have noticeable effects on *pax2a* expression (98% of injected embryos, *n*=30; Fig. 11C). Remarkably, knockdown of *sox32* and elimination of endoderm development in *osr1* morphants restored *pax2a* expression to a normal wild-type pattern (74% of injected embryos, *n*=66). To confirm these results, we tested whether reduction in endoderm development in the mutant *bonnie and clyde/mixer* (*bon*) would rescue the *osr1* loss-of-function phenotype. All embryos in an incross of *bon* heterozygotes showed a normal pattern of *pax2a* expression (Fig. 11E). Knockdown of *osr1* in embryos of an incross of *bon* heterozygotes resulted in the expected osr1 phenotype in roughly three quarters of the embryos (73%; Fig. 11F), whereas the remaining quarter (27%) of the clutch showed a normal rescued pattern of *pax2a* expression (Fig. 11G). Rescue of *pax2a* expression by *sox32* knockdown and the Mendelian ratio of *pax2a* rescued embryos in a *bon*+/– incross indicate that re-patterning of kidney versus vasculature in *osr1* morphants can be accounted for by expanded development of endoderm. A primary function of *osr1* may therefore be to pattern the mesendoderm during gastrulation.

DISCUSSION

The derivation of kidney and blood/vasculature from adjacent areas of mesoderm in developmental fate maps and the continued close association of progenitor cells during organogenesis (Crosier et al., 2002; Davidson and Zon, 2004; Fujimoto et al., 2001; Iraha et al., 2002; Kimelman, 2006; Kimelman and Griffin, 2000; Kimmel et al., 1990; Lane and Sheets, 2006; Vogeli et al., 2006; Walmsley et al., 2002) prompted us to examine whether genes acting during early development might affect the fate of both tissues. *osr1* has been reported to be expressed in the intermediate mesoderm and required for mouse and zebrafish kidney development (James et al., 2006; So and Danielian, 1999; Wang et al., 2005). Our data indicate that *osr1* is not simply required for kidney development but rather it acts early in development to pattern the mesendoderm that, in turn, has broader effects on development. Our results also show that in zebrafish, *osr1* is not expressed in typical intermediate mesoderm but rather in more lateral and ventral cells that may represent the zebrafish splanchnopleure (Funayama et al., 1999). We find that *osr1* expression in lateral cells (splanchnopleure) is not required for normal expression of *pax2a* as combined *sox32/osr1* loss of function results in normal *pax2a* expression. Unexpectedly, the primary mechanism underlying *osr1* loss-of-function phenotypes appears to be an increase in endoderm development that later acts to inhibit kidney and favor vascular cell differentiation in mesoderm.

A role for *osr1* in mesendoderm patterning

Mesoderm and endoderm are derived from a mixed population of cells, the mesendoderm, that constitutes the germ ring in zebrafish embryos. Our results suggest that expression of *osr1* in the germ ring plays an important role in mesendoderm patterning by acting as a repressor of endoderm formation. Both endoderm and mesoderm are induced by the Nodal-related factors *cyclops* and *squint* in zebrafish (Schier and Talbot, 2005). High levels of Nodal signals induce endoderm in the most marginal blastomeres, whereas in cells closer to the animal pole, induction of Tbox factors and FGF promote mesoderm development and antagonize endoderm development (Schier and Talbot, 2005). Ventral expression of BMPs has also been shown to antagonize endoderm development (Poulain et al., 2006). *osr1* expression is known to respond to BMP signaling in chick embryo mesoderm (James and Schultheiss, 2005) and we have confirmed that early expression of *osr1* in zebrafish requires the activity of a functional *bmp2b* gene (data not shown). One model of *osr1* activity would be that after induction by *bmp2b* signaling, *osr1* acts as a transcriptional repressor in mesendoderm cells (Tena et al., 2007), antagonizing transcriptional responses downstream of Nodal signaling (Schier and Talbot, 2005). However, the expression pattern of *osr1* throughout the germ ring suggests that, in addition to BMP signaling, *osr1* might also be responsive to FGF or nodal signaling (Rodaway et al., 1999). Further experiments examining signals upstream of *osr1* expression will be required to better define *osr1* function in the context of mesendoderm patterning.

Does altered mesendoderm patterning account for *osr1* phenotypes?

In mouse embryos, disruption of the *Osr1* gene causes severe defects in urogenital development (Wang et al., 2005). Mutant mice show no evidence of ureteric bud or metanephric kidney development and cellular defects in the Wolffian duct are evident at a very early stage (E8.5) (James et al., 2006; Wang et al., 2005). The nephrogenic mesenchyme shows reduced expression of *Wt1* (Wang et al., 2005) and also fails to express many other genes that define this tissue (James et al., 2006). The absence of properly specified nephrogenic mesenchyme in the mouse *Osr1* mutants, taken together with our results in the zebrafish raise the possibility that *Osr1* in the mouse may play additional roles outside of the nephrogenic mesoderm to ensure proper patterning of the intermediate mesoderm. Although *Osr1* expression in endoderm has not been detected in the mouse by in situ hybridization, recent analysis of a mouse *Osr1* (*Osr1*) bac transgenic shows that the *Osr1* gene contains regulatory elements that drive reporter expression (Cre) in endodermal organs (Grieshammer et al., 2008). Although suggestive of a function for *osr1* in endoderm, further experiments will be required to critically assess this possibility.

Our results differ from a previous study of *osr1* expression and function in zebrafish kidney development (Tena et al., 2007) where it was concluded that 'knockdown of *osr1* and *osr2* results in the loss of all pronephric structures including the glomerulus'. We find that *osr1* morphant kidney defects are restricted to the proximal nephron, and that glomerular morphogenesis is arrested in a stage-specific fashion, subsequent to podocyte *wt1a* expression. Our results are not due to a partial *osr1* loss of function as we demonstrate that no wild-type *osr1* mRNA can be detected by RT-PCR in *osr1* morphants at 24 hpf. These discrepancies are most probably due to the fact that Tena et al. did not examine *osr1* morphants with markers of the distal pronephros or the specification of glomerular podocytes by *wt1a* expression. In addition, in contrast to Tena et al., we show that zebrafish *osr1* is not expressed in *pax2a*-positive pronephric kidney cells during somitogenesis, nor in mature glomeruli. We observe *osr1* expression in cells adjacent to the forming pronephros at the 18-somite stage, which could have been easily mis-identified as the pronephros by Tena et al. In addition, we observe strong *osr1* expression in the liver, next to the glomerulus, at 48 hpf, which at low magnification may have been mistaken for glomerular expression by Tena et al. Our results agree with expression studies in the chick showing that *Osr1* is not expressed in differentiated kidney cells. Ectopic expression studies in the chick also support the idea that *osr1* expression may actually impede kidney epithelial differentiation (James et al., 2006).

Given the previous work on *osr1* and its broad early expression in the intermediate mesoderm, the segment-specific loss of kidney tissue and the selective expansion of vascular tissue in the anterior trunk of *osr1* morphants that we observed was unexpected. In addition, the fact that patterning defects in *pax2a*-positive kidney progenitors and *scl*-positive angioblasts were observed relatively

late in development, during somitogenesis, argues that *osr1* plays a role in maintenance, but not in specification, of mesodermal lineages. The simplest interpretation of our results is that signals that repress kidney and enhance angioblast development emanate from anterior endoderm and thus most strongly affect the anterior intermediate/lateral plate mesoderm. A central role for endoderm in the context of *osr1* loss of function may also help explain other phenotypes of *osr1* mutants/morphants. Both mouse and zebrafish embryos lacking *osr1* often show asymmetric loss of the Wolffian duct/pronephric duct on the left side (Wang et al., 2005) (our results), which has been interpreted to suggest the existence of a latent left-right asymmetry in the normally bilaterally symmetric kidney. Our results raise the alternative possibility that asymmetric loss of kidney tissue could be due to underlying asymmetries in endodermal tissues that negatively affect Wolffian/pronephric duct formation. Asymmetric defects in Wolffian duct development have also been reported in *Gata3* knockout mice (Grote et al., 2006), which might be due to cell-autonomous effects of *Gata3* loss of function in the Wolffian ducts. Interestingly, however, *Gata3* is also expressed in endodermal tissues (Caprioli et al., 2001; Debacker et al., 1999), which may indirectly affect kidney development.

Although we observed an increase in vascular tissue in *osr1* morphants, we did not observe a corresponding increase in blood cell development. This could be due to the fact that the most strongly affected tissue in *osr1* morphants, the anterior intermediate mesoderm, is known to be enriched for *flk*-and *scl*-positive angioblasts in zebrafish, whereas more posterior mesoderm contains both angioblasts and hematopoietic precursors that express *gata1* (Dooley et al., 2005). Alternatively, signals from expanded endoderm in *osr1* morphants may selectively favor angioblast development over erythropoiesis.

The role of the endoderm in mesodermal organogenesis

Our findings suggest that the effects of *osr1* loss of function on kidney and vascular patterning are mediated by signals from the endoderm. The endoderm is known to regulate the development of other mesodermal derivatives such as the heart (Alexander et al., 1999; Dickmeis et al., 2001; Kikuchi et al., 2000; Reiter et al., 1999). In chick and frog, the anterior endoderm induces cardiogenesis by secreting a combination of BMPs and soluble inhibitors of Wnt signaling such as Crescent and Dkk-1 (Marvin et al., 2001; Schneider and Mercola, 2001). In addition to its potential role as an inducer of heart tissue, endoderm provides a matrix upon which cardiac progenitors and angioblasts migrate to form a fused heart tube (Jin et al., 2005; Trinh and Stainier, 2004). Interestingly, lack of endoderm in the *one eyed pinhead* zebrafish mutant has been associated with a specific loss of vein, but not of aorta, development (Brown et al., 2000), which would be consistent with our results that an early expansion of endoderm expands vein but not aorta development. In the chick and mouse, sonic hedgehog signaling from endoderm is important for vasculogenesis (Vokes et al., 2004); however, this is apparently not essential in zebrafish (Jin et al., 2005). A candidate signal for the effect of endoderm on kidney development might be sonic hedgehog, as it is expressed in the endoderm and when expressed ectopically, hedgehog proteins can inhibit nephrogenesis (Urban et al., 2006). However, we found that cyclopamine treatment did not reverse the effects of *osr1* knockdown on kidney cell differentiation (Y.L. and I.D., unpublished), making it unlikely that hedgehog is the endoderm-derived signal. Thus, although these studies demonstrate that the endoderm is a rich source of soluble signaling molecules, it remains to be seen whether endoderm-derived soluble factors pattern kidney tissue in the IM.

In summary, our studies have uncovered a new role for *osr1* in patterning mesendoderm. *osr1* acts to inhibit endoderm differentiation during gastrulation. Our work has also uncovered a previously unknown role for endoderm in maintaining cell fate decisions in the intermediate mesoderm. Enhanced endoderm development favors the angioblast cell fate over kidney cell fate – presumably by non-cell-autonomous signals. Further identification of *osr1* primary target genes and the signals emanating from endoderm are likely to reveal important aspects of kidney and vascular progenitor cell differentiation.

We thank personnel in the Fish facility at MGH for help with fish husbandry, Dr Alan Davidson for the *swirl* mutant and for comments on this work, Dr Jing Wei Xiong for *bonnie and clyde* mutants and blood/vascular lineage markers, Randy Peterson and Chetana Sachidanandan for endoderm markers, Sasha Petrova for editing this manuscript, and Dr Tom Schultheiss for critical review of the data. This work was funded by a National Institute of Health grant (DK071041) to I.A.D. and by a postdoctoral fellowship from American Heart Association (0625923T) to S.P.M.

Supplementary material

Supplementary material for this article is available at
http://dev.biologists.org/cgi/content/full/135/20/3355/DC1

References

Alexander, J., Rothenberg, M., Henry, G. L. and Stainier, D. Y. (1999). casanova plays an early and essential role in endoderm formation in zebrafish. *Dev. Biol.* **215**, 343-357.

Barrallo-Gimeno, A., Holzschuh, J., Driever, W. and Knapik, E. W. (2004). Neural crest survival and differentiation in zebrafish depends on mont blanc/tfap2a gene function. *Development* **131**, 1463-1477.

Bisgrove, B. W., Raible, D. W., Walter, V., Eisen, J. S. and Grunwald, D. J. (1997). Expression of c-ret in the zebrafish embryo: potential roles in motoneuronal development. *J. Neurobiol.* **33**, 749-768.

Bollig, F., Mehringer, R., Perner, B., Hartung, C., Schafer, M., Schartl, M., Volff, J. N., Winkler, C. and Englert, C. (2006). Identification and comparative expression analysis of a second wt1 gene in zebrafish. *Dev. Dyn.* **235**, 554-561.

Bouchard, M., Souabni, A., Mandler, M., Neubuser, A. and Busslinger, M. (2002). Nephric lineage specification by Pax2 and Pax8. *Genes Dev.* **16**, 2958-2970.

Brown, L. A., Rodaway, A. R., Schilling, T. F., Jowett, T., Ingham, P. W., Patient, R. K. and Sharrocks, A. D. (2000). Insights into early vasculogenesis revealed by expression of the ETS-domain transcription factor Fli-1 in wild-type and mutant zebrafish embryos. *Mech. Dev.* **90**, 237-252.

Caprioli, A., Minko, K., Drevon, C., Eichmann, A., Dieterlen-Lievre, F. and Jaffredo, T. (2001). Hemangioblast commitment in the avian allantois: cellular and molecular aspects. *Dev. Biol.* **238**, 64-78.

Chen, J. N. and Fishman, M. C. (1996). Zebrafish tinman homolog demarcates the heart field and initiates myocardial differentiation. *Development* **122**, 3809-3816.

Chi, C. L., Martinez, S., Wurst, W. and Martin, G. R. (2003). The isthmic organizer signal FGF8 is required for cell survival in the prospective midbrain and cerebellum. *Development* **130**, 2633-2644.

Crosier, P. S., Kalev-Zylinska, M. L., Hall, C. J., Flores, M. V., Horsfield, J. A. and Crosier, K. E. (2002). Pathways in blood and vessel development revealed through zebrafish genetics. *Int. J. Dev. Biol.* **46**, 493-502.

Davidson, A. J. and Zon, L. I. (2004). The 'definitive' (and 'primitive') guide to zebrafish hematopoiesis. *Oncogene* **23**, 7233-7246.

Debacker, C., Catala, M. and Labastie, M. C. (1999). Embryonic expression of the human GATA-3 gene. *Mech. Dev.* **85**, 183-187.

Detrich, H. W., 3rd, Kieran, M. W., Chan, F. Y., Barone, L. M., Yee, K., Rundstadler, J. A., Pratt, S., Ransom, D. and Zon, L. I. (1995). Intraembryonic hematopoietic cell migration during vertebrate development. *Proc. Natl. Acad. Sci. USA* **92**, 10713-10717.

Dick, A., Hild, M., Bauer, H., Imai, Y., Maifeld, H., Schier, A. F., Talbot, W. S., Bouwmeester, T. and Hammerschmidt, M. (2000). Essential role of Bmp7 (snailhouse) and its prodomain in dorsoventral patterning of the zebrafish embryo. *Development* **127**, 343-354.

Dickmeis, T., Mourrain, P., Saint-Etienne, L., Fischer, N., Aanstad, P., Clark, M., Strahle, U. and Rosa, F. (2001). A crucial component of the endoderm formation pathway, CASANOVA, is encoded by a novel sox-related gene. *Genes Dev.* **15**, 1487-1492.

Dooley, K. A., Davidson, A. J. and Zon, L. I. (2005). Zebrafish scl functions independently in hematopoietic and endothelial development. *Dev. Biol.* **277**, 522-536.
Drummond, I. A., Majumdar, A., Hentschel, H., Elger, M., Solnica-Krezel, L., Schier, A. F., Neuhauss, S. C., Stemple, D. L., Zwartkruis, F., Rangini, Z. et al. (1998). Early development of the zebrafish pronephros and analysis of mutations affecting pronephric function. *Development* **125**, 4655-4667.
Elizondo, M. R., Arduini, B. L., Paulsen, J., MacDonald, E. L., Sabel, J. L., Henion, P. D., Cornell, R. A. and Parichy, D. M. (2005). Defective skeletogenesis with kidney stone formation in dwarf zebrafish mutant for trpm7. *Curr. Biol.* **15**, 667-671.
Fujimoto, T., Ogawa, M., Minegishi, N., Yoshida, H., Yokomizo, T., Yamamoto, M. and Nishikawa, S. (2001). Step-wise divergence of primitive and definitive haematopoietic and endothelial cell lineages during embryonic stem cell differentiation. *Genes Cells* **6**, 1113-1127.
Funayama, N., Sato, Y., Matsumoto, K., Ogura, T. and Takahashi, Y. (1999). Coelom formation: binary decision of the lateral plate mesoderm is controlled by the ectoderm. *Development* **126**, 4129-4138.
Gering, M., Rodaway, A. R., Gottgens, B., Patient, R. K. and Green, A. R. (1998). The SCL gene specifies haemangioblast development from early mesoderm. *EMBO J.* **17**, 4029-4045.
Gering, M., Yamada, Y., Rabbitts, T. H. and Patient, R. K. (2003). Lmo2 and Scl/Tal1 convert non-axial mesoderm into haemangioblasts which differentiate into endothelial cells in the absence of Gata1. *Development* **130**, 6187-6199.
Grieshammer, U., Agarwal, P. and Martin, G. R. (2008). A Cre transgene active in developing endodermal organs, heart, limb, and extra-ocular muscle. *Genesis* **46**, 69-73.
Grote, D., Souabni, A., Busslinger, M. and Bouchard, M. (2006). Pax 2/8-regulated Gata 3 expression is necessary for morphogenesis and guidance of the nephric duct in the developing kidney. *Development* **133**, 53-61.
Gupta, S., Zhu, H., Zon, L. I. and Evans, T. (2006). BMP signaling restricts hemato-vascular development from lateral mesoderm during somitogenesis. *Development* **133**, 2177-2187.
Habeck, H., Odenthal, J., Walderich, B., Maischein, H. and Schulte-Merker, S. (2002). Analysis of a zebrafish VEGF receptor mutant reveals specific disruption of angiogenesis. *Curr. Biol.* **12**, 1405-1412.
Hammerschmidt, M., Pelegri, F., Mullins, M. C., Kane, D. A., van Eeden, F. J., Granato, M., Brand, M., Furutani-Seiki, M., Haffter, P., Heisenberg, C. P. et al. (1996). dino and mercedes, two genes regulating dorsal development in the zebrafish embryo. *Development* **123**, 95-102.
Hans, S., Liu, D. and Westerfield, M. (2004). Pax8 and Pax2a function synergistically in otic specification, downstream of the Foxi1 and Dlx3b transcription factors. *Development* **131**, 5091-5102.
Hild, M., Dick, A., Rauch, G. J., Meier, A., Bouwmeester, T., Haffter, P. and Hammerschmidt, M. (1999). The smad5 mutation somitabun blocks Bmp2b signaling during early dorsoventral patterning of the zebrafish embryo. *Development* **126**, 2149-2159.
Humphrey, C. D. and Pittman, F. E. (1974). A simple methylene blue-azure II-basic fuchsin stain for epoxy-embedded tissue sections. *Stain Technol.* **49**, 9-14.
Iraha, F., Saito, Y., Yoshida, K., Kawakami, M., Izutsu, Y., Daar, I. O. and Maeno, M. (2002). Common and distinct signals specify the distribution of blood and vascular cell lineages in Xenopus laevis embryos. *Dev. Growth Differ.* **44**, 395-407.
James, R. G. and Schultheiss, T. M. (2005). Bmp signaling promotes intermediate mesoderm gene expression in a dose-dependent, cell-autonomous and translation-dependent manner. *Dev. Biol.* **288**, 113-125.
James, R. G., Kamei, C. N., Wang, Q., Jiang, R. and Schultheiss, T. M. (2006). Odd-skipped related 1 is required for development of the metanephric kidney and regulates formation and differentiation of kidney precursor cells. *Development* **133**, 2995-3004.
Jin, S. W., Beis, D., Mitchell, T., Chen, J. N. and Stainier, D. Y. (2005). Cellular and molecular analyses of vascular tube and lumen formation in zebrafish. *Development* **132**, 5199-5209.
Julich, D., Hwee Lim, C., Round, J., Nicolaije, C., Schroeder, J., Davies, A., Geisler, R., Lewis, J., Jiang, Y. J. and Holley, S. A. (2005). beamter/deltaC and the role of Notch ligands in the zebrafish somite segmentation, hindbrain neurogenesis and hypochord differentiation. *Dev. Biol.* **286**, 391-404.
Kikuchi, Y., Trinh, L. A., Reiter, J. F., Alexander, J., Yelon, D. and Stainier, D. Y. (2000). The zebrafish bonnie and clyde gene encodes a Mix family homeodomain protein that regulates the generation of endodermal precursors. *Genes Dev.* **14**, 1279-1289.
Kimelman, D. (2006). Mesoderm induction: from caps to chips. *Nat. Rev. Genet.* **7**, 360-372.
Kimelman, D. and Griffin, K. J. (2000). Vertebrate mesendoderm induction and patterning. *Curr. Opin. Genet. Dev.* **10**, 350-356.
Kimmel, C. B., Warga, R. M. and Schilling, T. F. (1990). Origin and organization of the zebrafish fate map. *Development* **108**, 581-594.
Kishimoto, Y., Lee, K. H., Zon, L., Hammerschmidt, M. and Schulte-Merker, S. (1997). The molecular nature of zebrafish swirl: BMP2 function is essential during early dorsoventral patterning. *Development* **124**, 4457-4466.
Kramer-Zucker, A. G., Wiessner, S., Jensen, A. M. and Drummond, I. A. (2005). Organization of the pronephric filtration apparatus in zebrafish requires Nephrin, Podocin and the FERM domain protein Mosaic eyes. *Dev. Biol.* **285**, 316-329.
Krauss, S., Johansen, T., Korzh, V. and Fjose, A. (1991). Expression of the zebrafish paired box gene pax[zf-b] during early neurogenesis. *Development* **113**, 1193-1206.
Lane, M. C. and Sheets, M. D. (2006). Heading in a new direction: implications of the revised fate map for understanding Xenopus laevis development. *Dev. Biol.* **296**, 12-28.
Leung, A. Y., Mendenhall, E. M., Kwan, T. T., Liang, R., Eckfeldt, C., Chen, E., Hammerschmidt, M., Grindley, S., Ekker, S. C. and Verfaillie, C. M. (2005). Characterization of expanded intermediate cell mass in zebrafish chordin morphant embryos. *Dev. Biol.* **277**, 235-254.
Liao, W., Bisgrove, B. W., Sawyer, H., Hug, B., Bell, B., Peters, K., Grunwald, D. J. and Stainier, D. Y. (1997). The zebrafish gene cloche acts upstream of a flk-1 homologue to regulate endothelial cell differentiation. *Development* **124**, 381-389.
Lieschke, G. J., Oates, A. C., Paw, B. H., Thompson, M. A., Hall, N. E., Ward, A. C., Ho, R. K., Zon, L. I. and Layton, J. E. (2002). Zebrafish SPI-1 (PU.1) marks a site of myeloid development independent of primitive erythropoiesis: implications for axial patterning. *Dev. Biol.* **246**, 274-295.
Liu, Y., Pathak, N., Kramer-Zucker, A. and Drummond, I. A. (2007). Notch signaling controls the differentiation of transporting epithelia and multiciliated cells in the zebrafish pronephros. *Development* **134**, 1111-1122.
Majumdar, A. and Drummond, I. A. (1999). Podocyte differentiation in the absence of endothelial cells as revealed in the zebrafish avascular mutant, cloche. *Dev. Genet.* **24**, 220-229.
Majumdar, A., Lun, K., Brand, M. and Drummond, I. A. (2000). Zebrafish no isthmus reveals a role for pax2.1 in tubule differentiation and patterning events in the pronephric primordia. *Development* **127**, 2089-2098.
Marcos-Gutierrez, C. V., Wilson, S. W., Holder, N. and Pachnis, V. (1997). The zebrafish homologue of the ret receptor and its pattern of expression during embryogenesis. *Oncogene* **14**, 879-889.
Marvin, M. J., Di Rocco, G., Gardiner, A., Bush, S. M. and Lassar, A. B. (2001). Inhibition of Wnt activity induces heart formation from posterior mesoderm. *Genes Dev.* **15**, 316-327.
Miller-Bertoglio, V., Carmany-Rampey, A., Furthauer, M., Gonzalez, E. M., Thisse, C., Thisse, B., Halpern, M. E. and Solnica-Krezel, L. (1999). Maternal and zygotic activity of the zebrafish ogon locus antagonizes BMP signaling. *Dev. Biol.* **214**, 72-86.
Nguyen, V. H., Schmid, B., Trout, J., Connors, S. A., Ekker, M. and Mullins, M. C. (1998). Ventral and lateral regions of the zebrafish gastrula, including the neural crest progenitors, are established by a bmp2b/swirl pathway of genes. *Dev. Biol.* **199**, 93-110.
Perner, B., Englert, C. and Bollig, F. (2007). The Wilms tumor genes wt1a and wt1b control different steps during formation of the zebrafish pronephros. *Dev. Biol.* **309**, 87-96.
Poulain, M., Furthauer, M., Thisse, B., Thisse, C. and Lepage, T. (2006). Zebrafish endoderm formation is regulated by combinatorial Nodal, FGF and BMP signalling. *Development* **133**, 2189-2200.
Pyati, U. J., Webb, A. E. and Kimelman, D. (2005). Transgenic zebrafish reveal stage-specific roles for Bmp signaling in ventral and posterior mesoderm development. *Development* **132**, 2333-2343.
Reiter, J. F., Alexander, J., Rodaway, A., Yelon, D., Patient, R., Holder, N. and Stainier, D. Y. (1999). Gata5 is required for the development of the heart and endoderm in zebrafish. *Genes Dev.* **13**, 2983-2995.
Rodaway, A., Takeda, H., Koshida, S., Broadbent, J., Price, B., Smith, J. C., Patient, R. and Holder, N. (1999). Induction of the mesendoderm in the zebrafish germ ring by yolk cell-derived TGF-beta family signals and discrimination of mesoderm and endoderm by FGF. *Development* **126**, 3067-3078.
Schier, A. F. and Talbot, W. S. (2005). Molecular genetics of axis formation in zebrafish. *Annu. Rev. Genet.* **39**, 561-613.
Schmid, B., Furthauer, M., Connors, S. A., Trout, J., Thisse, B., Thisse, C. and Mullins, M. C. (2000). Equivalent genetic roles for bmp7/snailhouse and bmp2b/swirl in dorsoventral pattern formation. *Development* **127**, 957-967.
Schneider, V. A. and Mercola, M. (2001). Wnt antagonism initiates cardiogenesis in Xenopus laevis. *Genes Dev.* **15**, 304-315.
Serluca, F. C. and Fishman, M. C. (2001). Pre-pattern in the pronephric kidney field of zebrafish. *Development* **128**, 2233-2241.
Shmukler, B. E., Kurschat, C. E., Ackermann, G. E., Jiang, L., Zhou, Y., Barut, B., Stuart-Tilley, A. K., Zhao, J., Zon, L. I., Drummond, I. A. et al. (2005). Zebrafish slc4a2/ae2 anion exchanger: cDNA cloning, mapping, functional characterization, and localization. *Am. J. Physiol. Renal Physiol.* **289**, F835-F849.
So, P. L. and Danielian, P. S. (1999). Cloning and expression analysis of a mouse gene related to Drosophila odd-skipped. *Mech. Dev.* **84**, 157-160.
Stickney, H. L., Imai, Y., Draper, B., Moens, C. and Talbot, W. S. (2007). Zebrafish bmp4 functions during late gastrulation to specify ventroposterior cell fates. *Dev. Biol.* **310**, 71-84.

Sumanas, S. and Lin, S. (2006). Ets1-related protein is a key regulator of vasculogenesis in zebrafish. *PLoS Biol.* **4**, e10.
Szeto, D. P. and Kimelman, D. (2004). Combinatorial gene regulation by Bmp and Wnt in zebrafish posterior mesoderm formation. *Development* **131**, 3751-3760.
Tena, J. J., Neto, A., de la Calle-Mustienes, E., Bras-Pereira, C., Casares, F. and Gomez-Skarmeta, J. L. (2007). Odd-skipped genes encode repressors that control kidney development. *Dev. Biol.* **301**, 518-531.
Thisse, B., Heyer, V., Lux, A., Alunni, V., Degrave, A., Seiliez, I., Kirchner, J., Parkhill, J. P. and Thisse, C. (2004). Spatial and temporal expression of the zebrafish genome by large-scale in situ hybridization screening. *Methods Cell Biol.* **77**, 505-519.
Thompson, M. A., Ransom, D. G., Pratt, S. J., MacLennan, H., Kieran, M. W., Detrich, H. W., 3rd, Vail, B., Huber, T. L., Paw, B., Brownlie, A. J. et al. (1998). The cloche and spadetail genes differentially affect hematopoiesis and vasculogenesis. *Dev. Biol.* **197**, 248-269.
Toyama, R. and Dawid, I. B. (1997). lim6, a novel LIM homeobox gene in the zebrafish: comparison of its expression pattern with lim1. *Dev. Dyn.* **209**, 406-417.
Trinh, L. A. and Stainier, D. Y. (2004). Fibronectin regulates epithelial organization during myocardial migration in zebrafish. *Dev. Cell* **6**, 371-382.
Urban, A. E., Zhou, X., Ungos, J. M., Raible, D. W., Altmann, C. R. and Vize, P. D. (2006). FGF is essential for both condensation and mesenchymal-epithelial transition stages of pronephric kidney tubule development. *Dev. Biol.* **297**, 103-117.
Vogeli, K. M., Jin, S. W., Martin, G. R. and Stainier, D. Y. (2006). A common progenitor for haematopoietic and endothelial lineages in the zebrafish gastrula. *Nature* **443**, 337-339.
Vokes, S. A., Yatskievych, T. A., Heimark, R. L., McMahon, J., McMahon, A. P., Antin, P. B. and Krieg, P. A. (2004). Hedgehog signaling is essential for endothelial tube formation during vasculogenesis. *Development* **131**, 4371-4380.
Walmsley, M., Ciau-Uitz, A. and Patient, R. (2002). Adult and embryonic blood and endothelium derive from distinct precursor populations which are differentially programmed by BMP in Xenopus. *Development* **129**, 5683-5695.
Wang, Q., Lan, Y., Cho, E. S., Maltby, K. M. and Jiang, R. (2005). Odd-skipped related 1 (Odd 1) is an essential regulator of heart and urogenital development. *Dev. Biol.* **288**, 582-594.
Westerfield, M. (1995). *The Zebrafish Book*. Eugene, OR: University of Oregon Press.
Wingert, R. A., Selleck, R., Yu, J., Song, H. D., Chen, Z., Song, A., Zhou, Y., Thisse, B., Thisse, C., McMahon, A. P. et al. (2007). The cdx genes and retinoic acid control the positioning and segmentation of the zebrafish pronephros. *PLoS Genet.* **3**, 1922-1938.